Journal of Catalysis **187,** 262–274 (1999)
Article ID jcat.1999.2599, available online at http://www.idealibrary.com on IDEAL®

Catalytic Conversion of N_2O to N_2 over Potassium Catalyst Supported on Activated Carbon

Z. H. Zhu and G. Q. Lu[1]

Department of Chemical Engineering, The University of Queensland, Queensland 4072, Australia

Received June 29, 1998; revised June 16, 1999; accepted June 17, 1999

Catalytic conversion of N_2O to N_2 with potassium catalysts supported on activated carbon (K/AC) was investigated. Potassium proves to be much more active and stable than either copper or cobalt because potassium possesses strong abilities both for N_2O chemisorption and oxygen transfer. Potassium redispersion is found to play a critical role in influencing the catalyst stability. A detailed study of the reaction mechanism was conducted based upon three different catalyst loadings. It was found that during temperature-programmed reaction (TPR), the negative oxygen balance at low temperatures (<50°C) is due to the oxidation of the external surface of potassium oxide particles, while the bulk oxidation accounts for the oxygen accumulation at higher temperatures (below ca. 270°C). N_2O is beneficial for the removal of carbon–oxygen complexes because of the formation of CO_2 instead of CO and because of its role in making the chemisorption of produced CO_2 on potassium oxide particles less stable. A conceptual three-zone model was proposed to clarify the reaction mechanism over K/AC catalysts. CO_2 chemisorption at 250°C proves to be an effective measurement of potassium dispersion.

Key Words: **potassium; catalyst; N_2O; activated carbon.**

INTRODUCTION

It is well known that alkali metal compounds catalyze the gasification of carbon or coal. Particularly, potassium is a good catalyst in carbon gasification and its catalytic role has been studied extensively (1–5). Recently, potassium has also been drawing increasing attention in nitric oxide catalytic conversion with carbon. Kapteijn *et al.* (6) observed a large increase in NO reduction (and carbon reactivity) when potassium was added to the carbon. Okukara *et al.* (7) found that, upon potassium addition to an activated carbon, both the NO adsorption capacity and carbon reactivity increased. Illán-Gómez *et al.* (8, 9) studied NO reduction by potassium loaded activated carbon in detail, and found that, similar to the carbon gasification by CO_2 or O_2, the catalytic role of potassium was also attributed to its effective participation in an oxidation-reduction (redox) cycle between K_xO_y and K_xO_{y+1}, in which the catalyst is oxidized by NO and reduced by carbon. Here K_xO_y is a substoichiometric oxide, in which the O/K ratio is lower than that of K_2O.

N_2O is an intermediate of the NO-carbon reaction (8, 9), and its reduction by carbon is also a carbon gasification reaction. So it is expected that potassium can catalyze N_2O reduction by carbon. Pels (10) found that it was very difficult to determine the reaction rates of sodium or potassium-impregnated Norit carbon with N_2O under fluidized-bed combustion conditions because of the very high activity. However, no report has been found on N_2O reduction by potassium-loaded carbon at lower temperatures (less than 400°C). As has been known (11–14), the identified anthropogenic sources of N_2O include not only low concentrations of N_2O from fossil fuel and biomass combustion but also high concentrations of N_2O (ca. 20–30%) from adipic acid production for Nylon 66 as well as nitric acid manufacture. Therefore it is necessary to develop catalytic processes to decompose N_2O at low temperatures. The studies on the catalytic decomposition of N_2O at low temperatures have so far concentrated on oxide supported catalysts. Catalysts for N_2O heterogeneous decomposition include (i) metals, like Pt and Au, (ii) pure oxides (CuO, Co_3O_4, etc.), and (iii) mixed oxides (perovskite types, exhydrotalcites). The supports can be alumina, silica, or zirconia, and zeolites. Excellent catalytic activities have been achieved on zeolite supported catalysts (15). Activated carbon is a very common and effective support as well as a reductant. In contrast to other inorganic carriers, it has a number of advantages: first, the active species are relatively facile to recover, which is important to precious metals. The second advantage is the carbon active sites, which can affect the catalytic activity. Its porous structure is useful to the formation of a highly dispersed catalyst active phase. Finally, the choice of catalysts may be much more flexible. In our previous study (16), a comparative study of N_2O decomposition over Cu/AC and Co/AC was made. This paper presents the results of N_2O catalytic conversion to N_2 over potassium loaded activated carbon.

[1] To whom correspondence should be addressed. E-mail: maxlu@cheque.uq.edu.au. Fax: 61 7 33654199.

0021-9517/99 $30.00

EXPERIMENTAL

Catalyst Preparation

The catalysts were prepared by impregnating activated carbon (Calgon BPL) with an aqueous solution of potassium nitrate (Ajax Chemicals, AR grade) at room temperature for 24 h. The sample was then dried by drying at ca. 100°C overnight and finally decomposed at 300°C in He for 1 h. The catalysts prepared with K loadings of 5, 10, and 20% were designated K-5/AC, K-10/AC, and K-20/AC, respectively. Generally, catalysts with any potassium loading were referred to as K/AC, and the parent activated carbon without any potassium as AC.

Catalyst Activity Measurements

The N_2O carbon reaction was carried out under atmospheric pressure in a fixed-bed flow reactor (10.0 mm inside diameter; 200 mg sample), and gaseous products were analyzed with a gas chromatograph (Shimadzu GC-17A) equipped with a heat conductivity detector and a Carbosphere column. Two modes of experiments were employed: (i) temperature-programmed reaction (TPR), in which the sample was first subjected to an *in situ* heat treatment in He at 25°C/min to 500°C and kept there for 1 h, then the temperature was lowered to room temperature followed by heating the sample at 4°C/min to ca. 400°C in a N_2O/He mixture; and (ii) isothermal reaction at 350°C. The feed gas, with a gas hourly space velocity (GHSV = 22500 ml g^{-1} h^{-1}), contained 3000 ppm N_2O in He. The particle size is 0.4–0.85 mm in isothermal reactions, and <0.08 mm in TPR experiments.

Specific Surface Area and Pore Volume Measurements

The N_2 adsorption/desorption isotherms at −196°C were obtained using a gas sorption analyzer (Quantachrome, NOVA 1200). Samples were degassed for 3 h at 300°C prior to the adsorption analysis. The BET surface area and total pore volume were obtained from the adsorption isotherms. The *t*-plot method was used to calculate the micropore surface area and micropore volume. CO_2 adsorption at 0°C was made with the same analyzer. The DR method was used to calculate the surface area and volume of micropores.

CO_2 Chemisorption and Thermal Decomposition of Catalysts

Thermogravimetric (TGA) experiments were carried out in a thermobalance (Shimadzu TGA-50). Samples were loaded into a platinum pan and heated under helium from room temperature to 110°C and held at this temperature for 20 min, and then heated to 900°C with a heating rate of 10°C/min to obtain a decomposition profile of the K catalyst, or to 500°C and kept for 1 h, followed by CO_2 chemisorption at 250°C. The procedure of CO_2 chemisorption was described in detail by IIlán-Gómez *et al.* (8).

RESULTS

Isothermal Reaction

A comparison of N_2O conversion over AC and K/AC catalysts is given in Fig. 1. N_2O conversion over pure AC is negligible at 350°C. Impregnation of K improves the activity substantially, and the activities are affected by both catalyst loading and heat treatment temperature. Samples heat-treated at 500°C show higher activities initially, and then drop to constant levels. With increasing K loading from 5 to 20%, both activity and stability of the catalysts increase. K5/AC shows a 97% N_2O conversion initially, and then quickly drops to a steady level of ca. 70%; K10/AC exhibits a 100% conversion for 30 min and then levels off at ca. 90%. For K20/AC, 100% conversion lasts ca. 80 min before reaching a final stable conversion level of ca. 97%. For K/AC catalysts subjected to 300°C heat treatment, the constant levels of conversion are almost the same as those of the samples subjected to 500°C heat treatment. Interestingly, the initial conversion was relatively lower for K20/AC and the conversion increased a bit during the period of reaction.

As carbon is not only a support, but also a reactant in each run, its consumption may reduce the reaction rate. In the present study, the weight loss of carbon is no more than 4.5% during the whole 150-min isothermal reaction even at 100% of N_2O conversion. It is seen that K20/AC showed the highest carbon consumption (due to the highest N_2O conversion) but the best stability. In contrast, the slightest

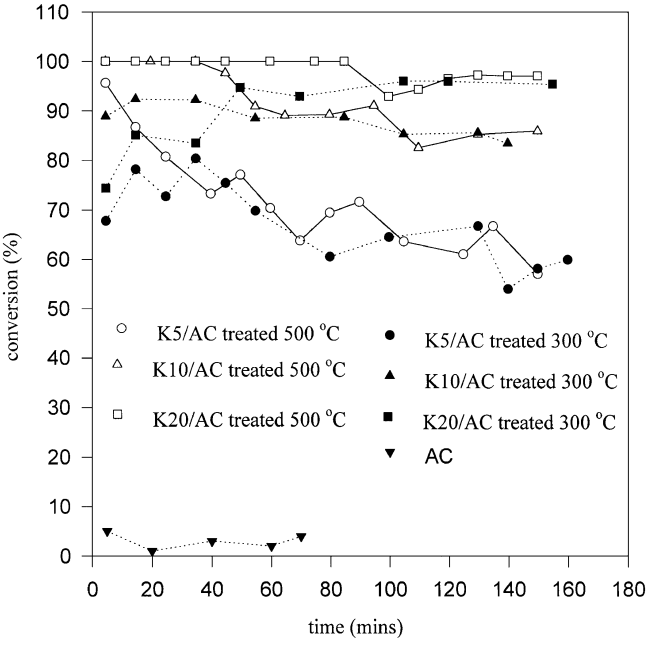

FIG. 1. N_2O conversion as a function of reaction time over K/AC (reaction conditions: $T = 350$°C, $P = 1$ atm, GHSV = 22500 ml g^{-1} h^{-1}, N_2O (in He) = 3000 ppm, particle size = 0.4–0.85 mm).

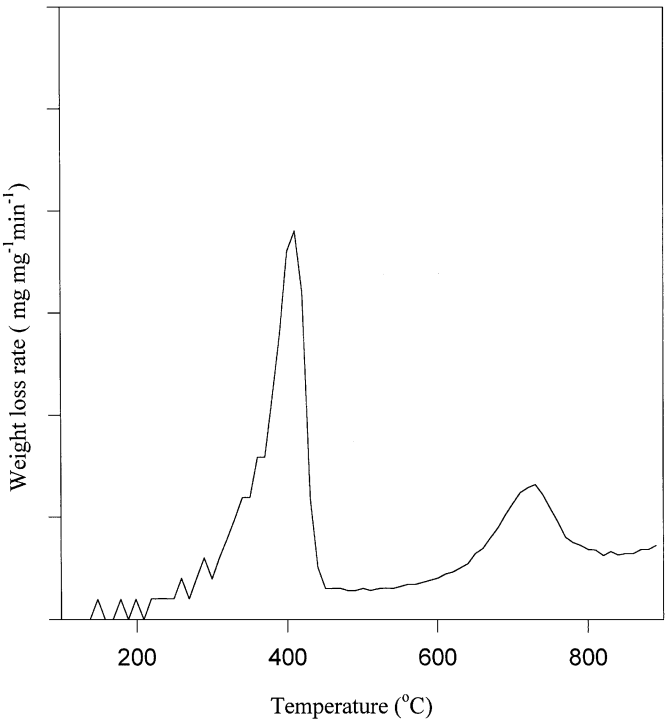

FIG. 2. Thermal decomposition curve of K20/AC obtained from TGA.

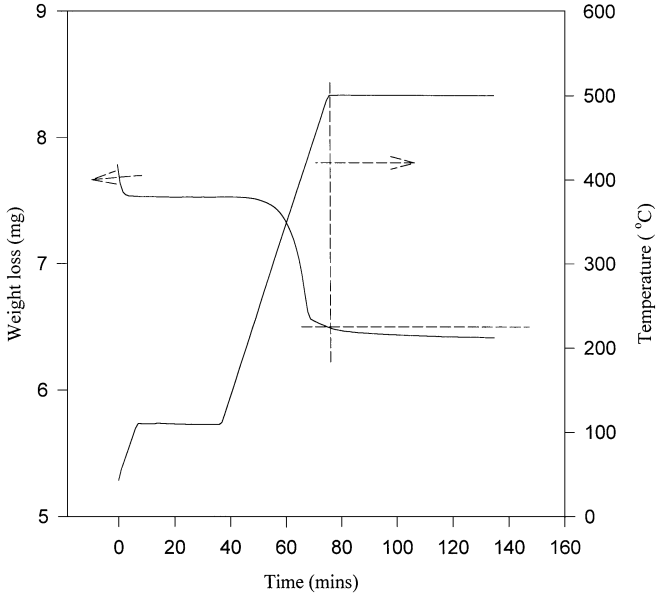

FIG. 3. Weight loss of K20/AC during 500°C heat treatment in helium.

carbon consumption was observed on K5/AC, which, however, showed the poorest stability. The following analysis will show that the stability of the catalysts depends mainly on the oxidation state of the catalyst particles instead of the carbon consumption. Indeed, no more than 4.5% of carbon consumption can be ignored during the whole 150-min isothermal reaction.

The different patterns of activity change caused by different heat treatment histories of the K/AC catalysts can be explained by the thermal decomposition curve of K20/AC obtained by TGA (see Fig. 2). There is a sharp peak around 400°C, which indicates the decomposition of KNO_3 into potassium oxides, and a broad peak between 600 and 800°C, which means the reduction of potassium oxides by activated carbon, and the reduction is weak before 600°C. As has been noted, the catalytic role of potassium in carbon gasification is actually through a redox cycle between K_xO_y and K_xO_{y+1}. This mechanism also applies in N_2O-carbon reaction. Upon heat treatment at 300°C, there was not much KNO_3 decomposed to potassium oxides (see Fig. 2). This is possibly why the N_2O conversion is relatively low initially for K20/AC. In contrast, 500°C heat treatment decomposes KNO_3 readily to potassium oxides. From Fig. 3, during the 500°C heat treatment in helium for 1 h, K20/AC shows a continuous weight loss, which is much larger than that of pure activated carbon (negligible for pure AC). This indicates that, during the heat treatment the potassium oxides formed have been further reduced by carbon into K_xO_y, which possesses a stronger ability for chemisorption, as observed in Fig. 1. As the N_2O-carbon reaction proceeds, K_xO_y becomes more oxidized, thus resulting in a reduced activity.

A comparison of activities over K20/AC, Cu20/AC, and Co20/AC (16) under the same experimental conditions is given in Fig. 4. After a 500°C heat treatment, the dynamic activity over Co20/AC is similar to that over K20/AC, but the stability of Co20/AC is much poorer than that over

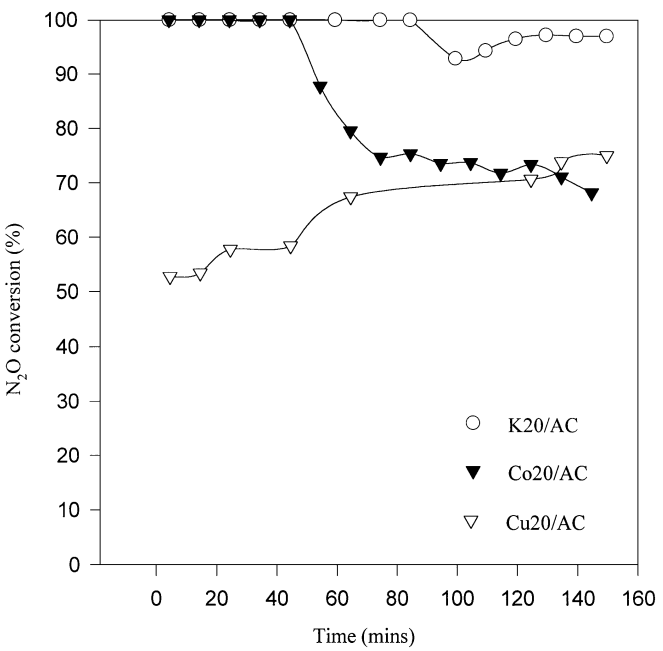

FIG. 4. A comparison of activities over K20/AC, Cu20/AC, and Co20/AC (reaction conditions: $T = 350$°C, $P = 1$ atm, GHSV = 22500 ml g^{-1} h^{-1}, N_2O (in He) = 3000 ppm, particle size = 0.4–0.85 mm).

K20/AC. Over Cu20/AC, the activity is initially lower, followed by a gradual increase, and the stable level is also much lower than that over K20/AC, but very close to that over Co20/AC. From our previous study (16), the catalytic role of Co or Cu is also through a redox cycle. Co is an easy acceptor of oxygen, resulting in the initial high activity. However, its poor ability for oxygen transfer from Co to carbon led to its quick deactivation in activity. Although Cu possesses a strong ability for oxygen transfer from Cu to carbon, it is a poor acceptor of oxygen, which may limit its activity. Cu^0 is less active than Cu^{+1}. The former was produced by the 500°C heat treatment in helium, and the latter resulted from the N_2O–carbon reaction process. This is why a gradual increase in the activity of Cu20/AC was observed during the 150-min isothermal reaction. The excellent activity of K/AC catalysts indicates that not only is the potassium catalyst an easy acceptor of oxygen but it also possesses a strong ability for oxygen transfer. Therefore potassium is much more active than Cu and Co.

Temperature-Programmed Reaction (TPR) Study

It is noted that in the above isothermal reaction, there is a significant internal diffusion resistance due to the large particle size (0.4–0.85 mm). In the TPR experiments, the activated carbon particles were further ground to less than 80 μm. The Weisz Criterion was calculated to be 0.015 (much less than 0.3) even for 100% conversion over K20/AC, indicative of the negligible internal diffusion limitation. We also found that at GHSV of 22500 ml g^{-1} h^{-1}, the external diffusion limitation is also eliminated as the N_2O pressure difference between the bulk and that on the surface of K20/AC particles was calculated to be 4.8×10^{-10} atm. Moreover, the temperature difference through the reaction bed was measured to be less than 0.5°C. Therefore, heat transfer resistance is also negligible under the experimental conditions.

Temperature-programmed reaction (TPR) profiles of N_2O–carbon on pure activated carbon (AC) and K/AC catalysts are shown in Fig. 5. No obvious reaction is observed over pure activated carbon until ca. 440°C, and the temperature required to reach 100% of N_2O conversion (T_{100}) is over 600°C. The impregnation of K caused a substantial decrease both in the starting reaction temperature and the T_{100}. For 20 wt% of K loading, vigorous reaction is found at ca. 150°C and 100% N_2O conversion is obtained at ca. 370°C. An increase in K loading shifts the TPR curves towards lower temperatures. However, the shape of TPR curves has not changed significantly. For the three K/AC samples, the following reaction regions are generally observed: (i) Before 150°C, a strong fluctuation in N_2O conversion is observed, but the conversion is low. The fluctuation may be related to the combination of dissociative chemisorption, nondissociative chemisorption, and physical adsorption. One other reason may be that the experimental system is not completely stable at this stage. (ii) Between 150 and 250°C, there is a larger N_2O decomposition peak. The higher the loading, the higher the peak is. (iii) From ca. 250°C, N_2O conversion increases almost linearly with temperature until 100% N_2O conversion is reached at ca. 370°C. The N_2O conversion during TPR is closely related to the state of the catalyst, and the mechanism will be discussed later, based upon a detailed analysis of TPR products.

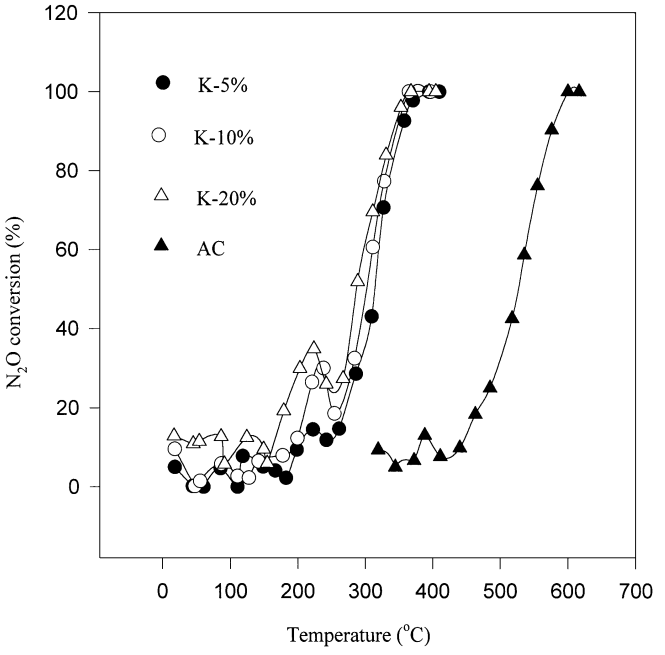

FIG. 5. Temperature-programmed reaction (TPR) profiles for N_2O reduction by K/AC and AC (reaction conditions: $P = 1$ atm, GHSV = 22500 ml g^{-1} h^{-1}, N_2O (in He) = 3000 ppm, particle size <0.08 mm).

According to the literature (16, 17), the N_2O–carbon reactions can be described as a first-order reaction with respect to N_2O. In this study, the height of the fixed bed is over 30 times the size of the particles, so the microreactor operation can be regarded as a plug flow. Furthermore, in each TPR experiment, the consumption of carbon is less than 2%; the influence of carbon consumption on reaction rate is negligible. As integral reactor instead of differential reactor was used in the present study, the reaction rate can not be calculated directly. For a first-order reaction, the reaction rate constant k can be calculated as

$$k = -\frac{F_0}{[N_2O]_0 W} \ln(1 - X), \qquad [1]$$

where F_0 is the molar N_2O feed rate, $[N_2O]_0$ is the molar N_2O concentration at the inlet, W is the catalyst amount, and X is the fraction N_2O conversion. The catalyst amount W is expressed in grams rather than in surface area since the true surface of the potassium catalyst (which is not the

BET surface for the carbon material) is not known. To the best of our knowledge, no proper method is available for the measurement of the surface area of potassium loaded in carbon, so far. The study followed will illustrate that the activity of potassium catalysts could be well normalized by CO_2 chemisorped at 250°C. The initial reaction rate of N_2O conversion R_0 (i.e., the rate at the inlet of the catalyst bed) can then be calculated:

$$R_0 = [N_2O]_0 k = -\frac{F_0}{W} \ln(1 - X). \qquad [2]$$

It should be mentioned here that at very high conversions the specific activity provides no fundamental rate because the state of the front end of the catalyst bed at low conversions could be much different from that in the back portion after most N_2O is converted. Thus, in the following analysis of the reaction rate during TPR, the running conversions close to 100% are not used.

The Arrhenius plots over K/AC catalysts and pure AC are compared in Fig. 6a. The reaction rate is greatly increased with an increasing K loading from 0 to 20%. Although the internal and external diffusion resistances are negligible, we still regard the activation energies obtained from TPR as apparent activation energies instead of intrinsic activation energies because the valence of potassium in potassium oxides was changing constantly during the TPR. The apparent activation energy is calculated to be 111.5 kJ/mol for AC, and other three samples have almost the same activation energy of ca. 76 kJ/mol, despite their different K loadings.

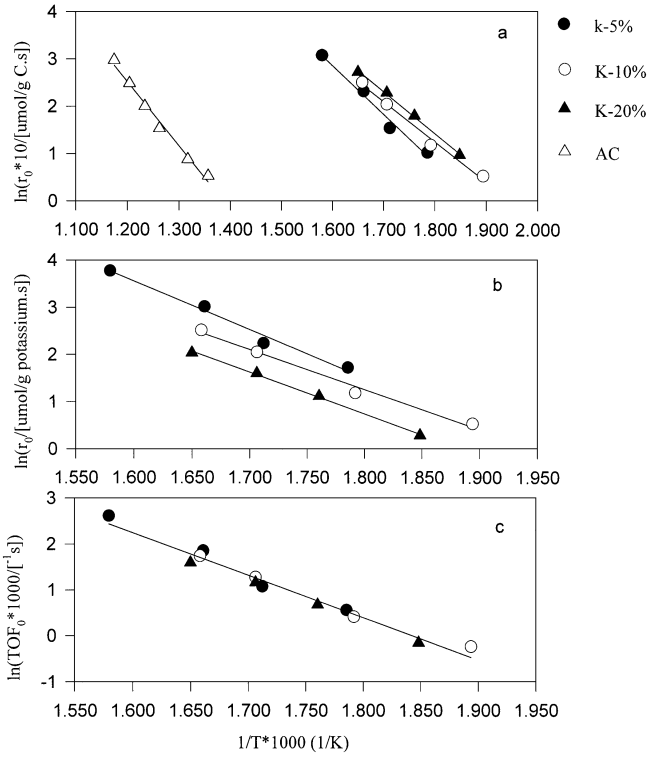

FIG. 6. (a) Arrhenius plots for N_2O conversion over AC and K/AC, (b) Arrhenius plots normalized by the loading of K, and (c) turnover frequencies based upon CO_2 chemisorbed at 250°C.

TABLE 1

Results of CO_2 Chemisorption on K/AC Catalysts

Samples	CO_2 Adsorped (μmol/g of sample)	CO_2/K_2O
K-5%	159.32	0.248
K-10%	216.75	0.169
K-20%	311.71	0.129
AC	—	—

Arrhenius plots normalized by the weight percentage of K (see Fig. 6b) show that an increase in K loading leads to the decrease of specific activity per gram K, indicating decreasing catalyst dispersion.

Chemisorption of CO_2 at 250°C was conducted after a heat treatment at 500°C in helium for 1 h and the results are shown in Table 1. For the convenience of analysis, we assume that one CO_2 can be adsorbed on one K_2O site to form the surface carbonate although, from our earlier discussion, it is substoichiometric K_xO_y instead of K_2O actually obtained. A decreasing ratio of CO_2/K_2O with increasing K loading is observed (column 3 in Table 1), which confirms the decreasing dispersion with K loading. This is consistent with the results in Fig. 6b. Turnover frequencies based upon CO_2 chemisorped at 250°C (μmol CO_2/g of sample) are shown in Fig. 6c. It is seen that nearly all data points of turnover frequencies fall onto a single line. This actually suggests that CO_2 chemisorption at 250°C is very effective for characterization of the dispersion of K catalyst supported on carbon. A more detailed argument about the dispersion of potassium catalyst will be made in the discussion section.

As has been noted, during the isothermal reactions in Fig. 1, the stable levels of N_2O conversion are the same despite that potassium catalysts heat-treated at 500°C presented a high initial activity and 300°C heat treatment showed a relatively low initial activity. We calculated the turnover frequencies at the stable levels of N_2O conversion (70% for K5/AC, 90% for K10/AC, and 97% for K20/AC). It is found that the turnover frequencies increase with an increase in catalyst loading (0.0063 s^{-1} for k5/AC, 0.0088 s^{-1} for K10/AC, and 0.0094 s^{-1} for K20/AC). This is completely contradictory to the results from the TPR experiments. Obviously, the internal diffusion limitation during isothermal reactions could not account for this contradiction because the turnover frequencies should decrease with the increasing catalyst loading if the diffusion limitation played a critical role. The reason could be the too-high N_2O conversions during the isothermal reactions (close to 100% for K20/AC

and K10/AC) which provide no fundamental data (as mentioned above) and would complicate the whole analysis. Therefore, we make no further attempt to analyze in detail the TOF data for results presented in Fig. 1.

Surface and Pore Structure

The surface area and pore structure data of all catalysts are listed in Table 2. AC and K/AC samples are predominately microporous, and increasing loading of K causes a tremendous decrease in surface area and pore volume. Because the collapse of the pore structure of activated carbon at 500°C in helium proves to be impossible, the decrease in surface area and pore volume must result from the blockage of pores by the small potassium oxide particles. From column 5 in Table 2, $V_{m\text{-}N2}/V_t$, the ratio of mircropore volume obtained from N_2 adsorption to the total pore volume, decreases with increasing K loading. It can be deduced that the distribution of K catalyst is not completely uniform and more micropores have been blocked than mesopores. It is well known that N_2 and CO_2 do not measure the same type of microporosity (18). CO_2 gives the micropores ($V_{mi\text{-}CO2}$), and N_2 the total micropore volume ($V_{mi\text{-}N2}$) including the supermicropores (18, 19). The volume of supermicropores (V_{sp}) can be determined as the difference between $V_{mi\text{-}N2}$ and $V_{mi\text{-}CO2}$. It is seen that (from column 8, Table 2) the impregnation of potassium generally results in the decrease in $V_{mi\text{-}CO2}/V_{sp}$, which means that more potassium oxide particles are located in $V_{mi\text{-}CO2}$ than in V_{sp}.

Figure 7 shows the stability of activity of K20/AC and the change in surface area during the 540-min isothermal reaction at 350°C (the catalyst was subjected to a heat treatment in He at 500°C before reaction). After the 150-min reaction, N_2O conversion drops to ca. 97% from 100%, while the surface area rises to 690 m^2/g from 646 m^2/g. In the remaining time, the N_2O conversion keeps nearly constant despite the significant decrease by more than 30% in the surface area of K20/AC. Therefore the activity of this K/AC catalyst is not proportional to the surface area. It is also noted that carbon consumption during the 540-min isothermal reaction is ca. 16%, while the activity of K20/AC just decreased by 3%. This further confirms the above conclusion that the stability of K/AC depends mainly on the nature of catalyst particles, and the influence of carbon consumption can be ignored.

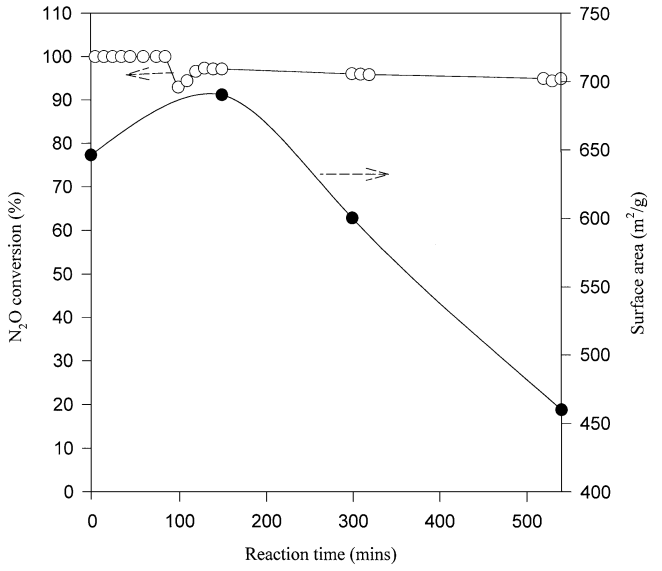

FIG. 7. Stability of activity and variation in specific surface area (reaction conditions: reaction $T = 350°C$, $P = 1$ atm, GHSV = 22500 ml g^{-1} h^{-1}, particle size = 0.4–0.85 mm).

From column 5 in Table 2, the ratio of $V_{m\text{-}N2}/V_t$ remains almost unchanged inspite of the noticeable increase in total pore volume within the initial 150 min, which means that the increase in $V_{m\text{-}N2}$ is proportional to V_t during this period. However, in the remaining 390 min, $V_{m\text{-}N2}/V_t$ keeps increasing inspite of the decrease in total pore volume (see column 8, Table 2). A continuous increase in $V_{m\text{-}CO2}/V_{sp}$ is observed during the whole 540-min reaction period. This provides useful information for the later discussion on the redispersion of K.

TABLE 2

Specific Surface Area and Pore Volume of Catalysts (Size 0.4–0.85 mm)

Sample	S (m^2/g)	V_t (cc/g)	$V_{m\text{-}N2}$ (cc/g)	$V_{m\text{-}N2}/V_t$	$V_{m\text{-}CO2}$	V_{sp} (cc/g)	$V_{mi\text{-}CO2}/V_{sp}$
AC	1077	0.511	0.408	0.7996	0.236	0.172	1.372
K5/AC	898	0.436	0.340	0.7798	0.195	0.145	1.344
K10/AC	803	0.397	0.301	0.7582	0.158	0.143	1.105
K20/AC	646	0.341	0.247	0.7269	0.130	0.117	1.11
K20/AC1	690	0.370	0.268	0.7245	0.148	0.12	1.23
K20/AC2	600	0.310	0.238	0.7660	0.135	0.103	1.31
K20/AC3	460	0.232	0.184	0.7931	0.110	0.074	1.48

Note. S, BET specific area (m^2/g); K20/AC1, 150-min isothermal reaction at 350°C; K20/AC2, 300-min isothermal reaction at 350°C; K20/AC3, 540-min isothermal reaction at 350°C.

DISCUSSION

Reaction Mechanism

Analysis of TPR products provides important information on the reaction. Figure 8 shows the evolution of products during the TPR experiment over three K/AC catalysts. We found that the CO_2 selectivity defined as $100\% * CO_2/(CO_2 + CO)$ is 100% during the whole TPR experiments; i.e., no CO was detected in the products. Because one N_2O molecule reacting with carbon produces one N_2 but just 0.5 CO_2, the number of moles of N_2 is double that of CO_2 if no oxygen is retained on the surface. In order to better show the oxygen balance in the product analysis, the CO_2 concentration is multiplied by 2. In this way, CO_2

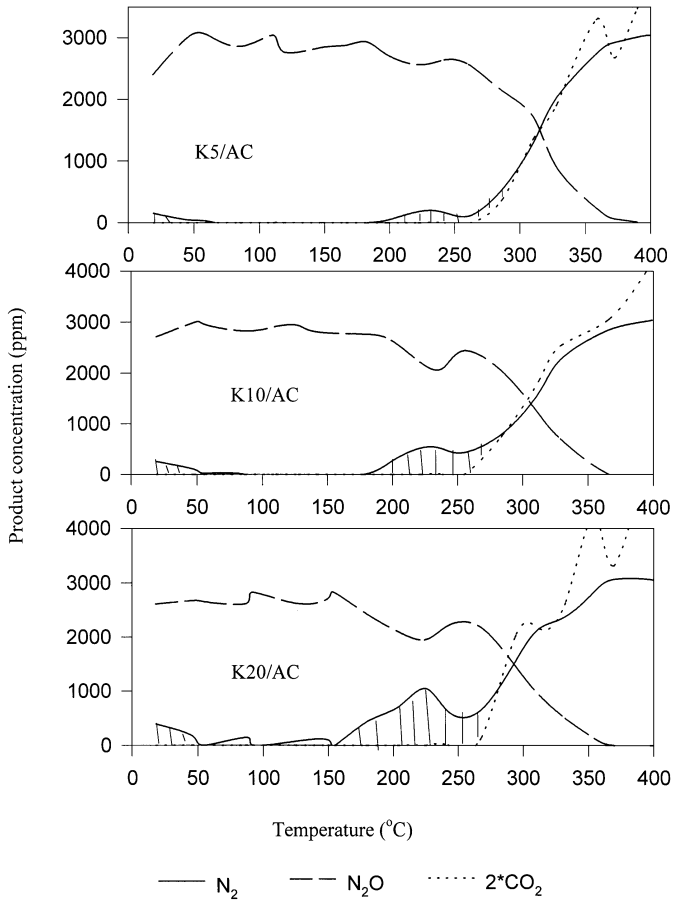

FIG. 8. Evolution of products during TPR over K/AC (CO_2 levels are doubled in this analysis).

concentration is equal to N_2 concentration in the products if there is no delay for oxygen-containing products. From Fig. 8, four regions of reactivity over K20/AC are observed:

(I) The first stage is characterized by the low conversion of N_2O and the very weak evolution of N_2 ($T <$ ca. 50°C). However, no oxygen-containing products other than N_2O are found, and oxygen from N_2O decomposition was retained on the K/AC catalyst. Obviously, this is due to an irreversible dissociative chemisorption of N_2O on potassium oxide particles, which was also observed on Ni (20) and Cu (21) at such a low temperature. Nondissociative chemisorption or physical adsorption can also be observed here from the negative N_2 balance.

(II) In the second stage (50°C < T < 150°C), chemisorption seems to be saturated, for N_2 almost disappears and N_2O conversion is negligible; no more oxygen accumulation occurs at this stage.

(III) In the third stage (150°C < T < 250°C), the N_2 peak reappears but is much stronger compared with that in the first stage. The oxygen balance is still negative in this stage, for no CO_2 is observed.

(IV) The fourth stage is characterized by the appearance of CO_2 at ca. 250°C, from which temperature N_2 starts to increase almost linearly until 100% N_2O conversion is reached at ca. 370°C. However, CO_2 increases more quickly than N_2 as an excess of CO_2 evolution with respect to N_2 is observed at ca. 270°C. So the oxygen balance is still negative below 270°C, but becomes positive afterwards.

Similar reaction stages are also observed over K10/AC and K5/AC except that the smaller N_2 peaks are observed because of the lower catalyst loadings. Considering the good activity of K20/AC, in the following analysis, we will mainly concentrate on K20/AC, unless otherwise stated.

An analysis of the oxygen balance provides important information for the reaction mechanism. As has been noted, during the 500°C heat treatment in helium for 1 h, the catalyst precursor was reduced by carbon to a substoichiometric oxide K_xO_y. In Fig. 8, during TPR, oxygen balance is negative in the first stage, the third stage, and the initial part of the fourth stage (below ca. 270°C for K20/AC). This negative oxygen balance indicates oxygen accumulation and formation of more oxidized K_xO_{y+1}. In the fourth stage, above ca. 270°C over K20/AC, oxygen balance becomes positive, indicating the release of oxygen accumulated in the previous stages. As the surface complexes remaining on the carbon surface following the initial 500°C heat treatment can also be released far below 500°C in the presence of N_2O atmosphere, it is hard to make a quantitative calculation of the positive oxygen balance. However, it is indeed possible to make a estimation of the negative oxygen balance. In Fig. 8, negative oxygen balance is shown by shaded areas, and a quantitative summary of oxygen accumulation on a per gram of K basis is presented in Table 3, from integration of these areas. Figure 8 shows that the negative oxygen balance areas in the third and fourth stages are continuous. So we lumped them together as given in column 3 of Table 3. The following observations are made:

(I) The oxygen accumulated per gram of K is much less in the first stage (column 2, Table 3) than that in the third and fourth stage (column 3, Table 3) over all three catalysts. We also note that chemisorption is much quicker in the former stage than in the latter stages.

TABLE 3

Oxygen Accumulation during TPR over K/AC Catalysts

Sample	O accumulated in stage I (μmol/g K)	O accumulated in stage III + IV (μmol/g K)	Total O accumulated (μmol/g K)
5K/AC	294	1237	1531
10K/AC	230	1444	1674
20K/AC	181	1494	1675

(II) For different catalysts, with the increase in catalyst loadings, oxygen accumulation per gram of K decreases in the first stage (column 2, Table 3); this trend corresponds to the catalyst dispersion based on CO_2 chemisorption. However, increasing catalyst loading improves oxygen accumulated in the latter stages (column 3, Table 3).

(III) The total oxygen accumulated before the positive oxygen balance keeps nearly constant despite different catalyst loadings (column 4, Table 3).

As N_2O chemisorption is most likely to occur on the external surface of K_xO_y particles, which is directly exposed to the N_2O atmosphere, it is suggested that the negative oxygen balance in the first stage is due to the oxidation of external surface of K_xO_y particles. This explains why chemisorption in the first stage finishes so quickly. However, oxygen transfer from the external surface to the bulk of K_xO_y particles is impossible at such low temperatures, so the chemisorption in the first stage is also very weak. This suggestion is further evidenced by the good agreement between the sequence of oxygen amounts accumulated in the first stage and that of CO_2 amounts chemisorbed at 250°C. With increasing temperature, oxygen retained on the external surface can gradually migrate into the bulk of K_xO_y particles or even to the interface of the catalyst–carbon contact, resulting in the negative oxygen balance in the third stage. At the same time, the external surfaces of catalyst particles become less oxidized and can thus chemisorb N_2O continuously. With the further increase in temperature, oxygen can even be transferred from the catalyst particles to carbon active sites. Consequently, CO_2 evolution is observed at ca. 250°C, which is considered as the start of the fourth reaction stage. But the oxygen balance is still negative until CO_2 catches up with N_2 at ca. 270°C. Afterwards the oxygen balance becomes positive. The assumption that the negative oxygen balance in the third and fourth stages is due to the gradual oxidation of bulk and interface of K_xO_y particles offers a good reason that chemisorption in the third stage is relatively slower but much stronger compared with that in the first stage. This assumption is further confirmed by observation III; i.e., the total oxygen accumulated per gram of K before the positive oxygen balance remains nearly the same for different catalyst loadings. Very interestingly, the positive oxygen balance in the fourth stage is also divided into two parts over three catalysts; it is relatively smaller below ca. 310°C, while greatly improved by a further increase in reaction temperature. As the oxygen transfer from catalyst to carbon active sites is most likely to take place on the interface, we think that the smaller excess of CO_2 is due to the release of oxygen near the catalyst–carbon interface at relatively lower temperatures, while the release of oxygen in the bulk or even the external surface of K_xO_y particles leads to the bigger positive oxygen balance above ca. 310°C.

According to the previous literature (10), N_2O favors the removal of surface carbon–oxygen complexes by the mechanism $C\text{–}(CO) + N_2O \rightarrow C_f + N_2 + CO_2$, here C_f is a produced active site. This is further confirmed by the 100% CO_2 selectivity (defined as $100\% * CO_2/(CO_2 + CO)$) during the whole TPR, as well as isotherm reactions in the present study, as the release of CO_2 needs lower activation energy than that of CO. However, because of the high thermodynamic propensity of potassium oxides to chemisorb CO_2, CO_2 evolved during TPR may be rechemisorbed on K_xO_y particles below 250°C; this may in turn affect N_2O chemisorption on K_xO_y. In order to investigate the effects of N_2O and CO_2 on each other, a special TPR was conducted as follows. After the initial 500°C heat treatment in He, the catalyst sample was cooled down to 170°C, at which 10% CO_2 was introduced and kept there for 10 min, followed by purging with pure He until no CO_2 was detectable in the outlet of the purging gas. Afterwards, the sample was further cooled down to room temperature, and then the usual TPR experiment was performed. The result of the special TPR is presented in Fig. 9. It is seen that due to the chemisorptin of CO_2 on the external surface of K_xO_y particles, the N_2 peaks in the first and the third stages disappear; thus N_2O chemisorption is significantly blocked by CO_2 chemisorbed at relatively low temperatures. On the other hand, CO_2 starts to evolve at ca. 130°C in the presence of N_2O although CO_2 prechemisorption was carried out at 170°C. This means that CO_2 prechemisorbed on the surface of K_xO_y becomes less stable in the presence of N_2O.

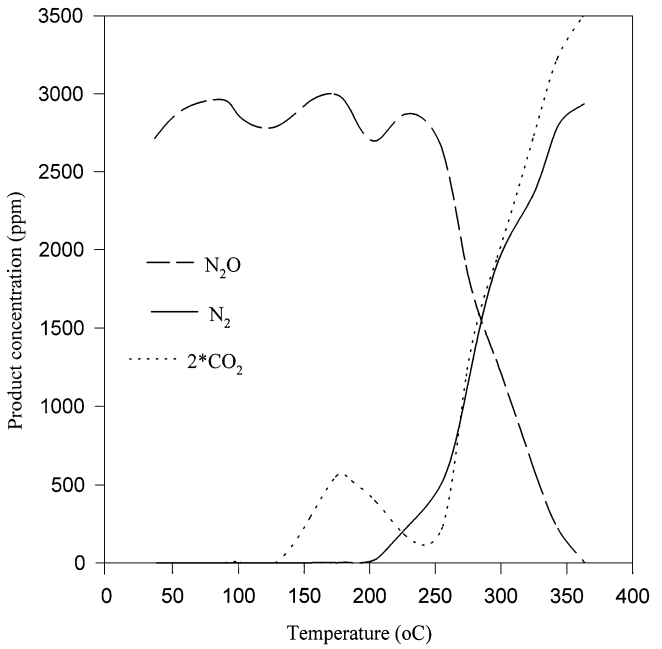

FIG. 9. Evolution of products during the special TPR (i.e., prechemisorption of CO_2 on K20/AC at 170°C prior to TPR) over K20/AC (CO_2 levels are doubled).

When the CO_2 evolution peak due to CO_2 prechemisorbed at 170°C approaches completion, N_2 appears at ca. 200°C, indicative of the start of N_2O dissociative chemisorption. From 250°C, both N_2 and CO_2 begin to increase linearly, resulting from a vigorous N_2O–carbon reaction catalyzed by the potassium catalyst. As N_2O dissociative chemisorption was blocked by prechemisorbed CO_2, little oxygen accumulated in the previous stages. This is why CO_2 does not exceed N_2 during the linear increase until the temperature rises to 300°C in the special TPR, compared with 270°C in the usual TPR. We also note that the vigorous CO_2 evolution from N_2O–carbon reaction started at ca. 250°C in both the special and usual TPR experiments. One can argue that the reason that no CO_2 was detected until ca. 250°C in the usual TPR (Fig. 8) is that CO_2 could be released from the carbon surface, and rechemisorbed on K_xO_y particles. If this assumption was true, CO_2 evolution from N_2O–C reaction catalyzed by potassium should have occurred at much lower temperatures (in the presence of N_2O) in the usual TPR than in the special TPR because a large amount of oxygen was accumulated below 250°C in the former while little accumulated in the latter. This assumption is obviously contrary to what was observed. Therefore, it is suggested that no (or negligible) CO_2 is released from the carbon surface below 250°C in the usual TPR because at such low temperatures, oxygen transfer from potassium to carbon is impossible, or oxygen could be transferred from potassium to carbon but the carbon–oxygen complexes could hardly decompose. Once the decomposition of carbon–oxygen complexes starts, the presence of N_2O makes CO_2 chemisorption on K_xO_y particles rather unstable; thus the produced CO_2 can quickly evolve into the products. Therefore, the influence of rechemisorption of CO_2 on N_2O-carbon reaction catalyzed by potassium is negligible (because of the presence of N_2O).

The mechanism of potassium catalyzed N_2O–carbon reaction is concluded as follows. Dissociative N_2O chemisorption can take place on the external surface of K_xO_y particles even at very low temperatures (<50°C). However, oxygen transfer requires a higher temperature. N_2O conversion will stop if oxygen cannot be transferred in time. With the increase in temperature, oxygen is transferred from the external surface to the bulk or even to the catalyst–carbon interface. The external surface then becomes less oxidized and N_2O chemisorption goes on. With further increases in temperature, oxygen can be transferred from potassium to carbon, followed by the decomposition of carbon–oxygen complexes. The N_2O atmosphere favors the removal of carbon–oxygen complexes not only by improving CO_2 selectivity but also by making CO_2 chemisorption less stable on potassium oxide particles. Because of the oxygen accumulation in the early stages, an excess of CO_2 with respect to N_2 is observed shortly. At low temperatures, the limiting factor is oxygen transfer, but at higher temperatures N_2O conversion may be limited by dissociative chemisorption. Obviously, the redox cycle between K_xO_y/K_xO_{y+1} in the previous studies (4, 5, 8) is too simple to explain the second delay of oxygen-containing products in the third and fourth stage; i.e., N_2 release is observed again at ca. 150°C, but CO_2 did not appear until above 250°C. Therefore, the hypothesis about the oxidation of the external surface and the bulk of catalyst particles in this study provides a more detailed and appropriate explanation of the reaction mechanism.

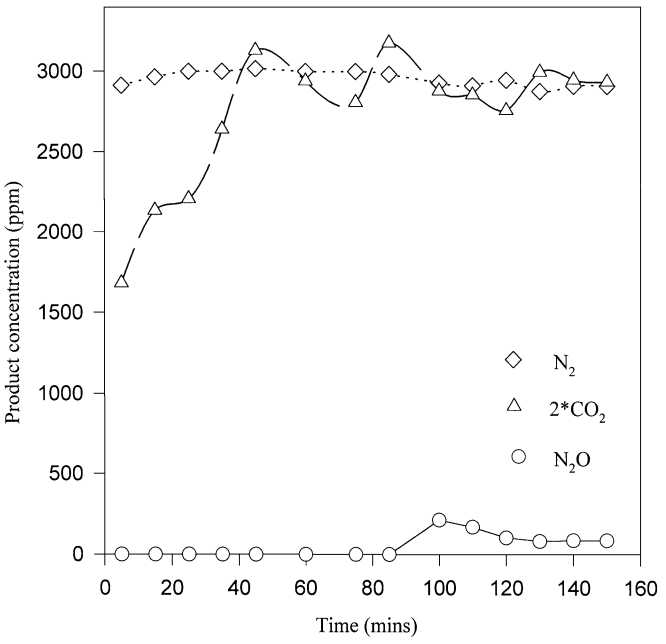

FIG. 10. Evolution of products during isothermal reaction at 350°C over K20/AC (the sample was subjected to heat treatment at 500°C in helium prior to the isothermal reaction, and CO_2 levels are doubled).

From Fig. 10, a delay in the evolution of CO_2 with respect to N_2 during the isothermal reaction at 350°C over K20/AC (subjected to 500°C heat treatment before reaction) lasts about 80 min, which corresponds to the duration for 100% N_2O conversion. Afterwards CO_2 keeps a good balance with N_2. This confirms the above redox cycle mechanism; i.e., initially, the K_xO_y produced by the 500°C heat treatment can accept further oxygen from N_2O and be more oxidized into K_xO_{y+1} gradually at 350°C. The 100% of N_2O conversion will continue until no more oxygen can accumulate on potassium oxides and such a redox cycle K_xO_y/K_xO_{y+1} has been built up. Nevertheless, the analysis of products during the isothermal reaction cannot provide enough details on the reaction mechanism.

Redispersion of Potassium

As has been noted, potassium shows much higher activity than either copper or cobalt in N_2O–carbon reaction. In the study of NO reduction over Cu/AC, Hu and Ruchenstein (22) found that the activity of Cu was substantially reduced

by heat treatment at a temperature higher than 300°C. Moreover they used a 450-min isothermal reaction at 330°C to study the stability of Cu20/AC and observed a noticeable deactivation. (Obviously, the activity variation of Cu20/AC in Fig. 4 can not be regarded as a correct evidence because of the short reaction time.) In both cases, sintering of copper was suggested to be the reason, whereas potassium shows strong resistance to sintering during either heat treatment or reaction. From Fig. 7, during the 540-min isothermal reaction, the surface area of K20/AC decreased by more than 30% and carbon was consumed by 16%, but the activity remained nearly constant. As seen from Fig. 1, the heat treatment in helium at 500°C produced more reduced K_xO_y species, thus resulting in much higher initial activity than that treated at 300°C, but the activities of the catalysts became the same after a period of time. It is clear that potassium catalysts exhibit both better activity and stability compared to Cu/AC and Co/AC catalysts. Moreover, the conditions required to prepare and treat the K/AC catalysts are not that critical since heat treatment does not alter the stable activity of the catalyst that much. Both the stability of activity and the flexibility in catalyst preparation are probably attributed to the nature of redispersion of potassium, which has been extensively studied previously for other gasification systems. By using the methylation technique, Mims *et al.* (23, 24) demonstrated the existence of surface salt complexes such as phenoxide groups, which allow the potassium to achieve high and reproducible dispersion on carbon. In the follow-up studies, Radovic *et al.* (25, 26) found that potassium can redisperse itself quite readily during gasification and the K-catalyzed gasification behavior is independent of the catalyst preparation method. Using a TPD technique, Kapteijn *et al.* (27) suggested that during alkali metal-catalyzed gasification in CO_2, two types of oxidic species are present, surface bonded-OM (here M is alkali metal) species of high stability and oxidic speicies that have less interaction with the carbon surface. This suggestion was confirmed by the results of Yang *et al.* (28, 29), who found that the surface species are mainly phenoxide groups, and the oxidic species are alkali clusters. The cluster is anchored to the carbon by phenoxide groups but is more active than the surface salt species. The intercalate-like structure of alkali catalysts caused by heat treatment or gasification further confirms the nature of redispersion of alkali metals.

In another study of NO with Cu/AC, Ruckenstein and Hu (30) observed a continuous decrease in the ratio of micropore volume to total pore volume and thus suggested that carbon oxidation occurs faster in micropores than in mesopores, resulting in more micropores consumed than mesopores. However, in the present study, an increasing ratio $V_{m\text{-}N2}/V_t$ from 150 to 540 min of reaction and a continuously increasing ratio $V_{m\text{-}CO2}/V_{sp}$ during the whole 540-min reaction over K20/AC were observed (Table 2). This indicates that although more micropores were consumed than mesopores in the reaction, K could migrate into the micropores through redispersion, thus producing new micropores continuously to compensate for the consumed micropores. It is by the same mechanism as that in KOH activation that micropores are being created. Differently, Cu is easy to sinter. Once Cu particles become bigger, they can not get back into the micropores any more, and the reproduction of new micropores is impossible, resulting in the decreasing ratio of micropore volume to total pore volume as more micropores are consumed, as reported by Ruckenstein and Hu (30).

CO_2 Chemisorption at 250°C

CO_2 chemisorption at 300°C has been attempted to measure the active site density of alkali catalysts on coal at intermittent periods of coal gasification, and a constant turnover number was obtained (31). The same method was also successfully used to characterize the external surface and the dispersion of calcium particles on carbon (32). However, Illán-Gómez and co-workers had a problem when they tried to use CO_2 chemisorption as a means to study the dispersion and active site density of potassium supported on activated carbon for NO reduction (8, 33). Their results are reproduced in Table 4.

In Table 4a, CO_2/K_2O decreases with decreasing K loading. This comparison makes no sense because the carbon supports are different. In Table 4b, CO_2/K_2O keeps almost constant in spite of the increasing K loading, which is contrary to our results in Table 1. However, the reason for this can be found by examining the heat treatment conditions in their work. The samples in Illán-Gómez and co-workers' study (8, 33) were subjected to a heat treatment at 900°C in helium, which could reduce potassium oxides into element potassium. Yokoyama and co-workers studied the decomposition of K_2CO_3 (34) in AC by XPS and found that K_2CO_3 decomposed into potassium oxides at 650°C in He, accompanied by the reduction of potassium oxides to elemental potassium, which could penetrate into

TABLE 4

Results of CO_2 Chemisorption on Ion-Exchanged Potassium-Loaded Carbon (8, 33)

Sample	CO_2 adsorbed (μmol/g of sample)	CO_2/K_2O
(a)		
A(ox)-4.9	289	0.46
B(ox)-3.9	160	0.32
K-UA1(ox)	137	0.15
(b)		
K-UA1	—	—
K-UA1-2.8	154	0.43
K-UA1-4.6	253	0.43
K-UA1-7.4	436	0.46

the bulk carbon until no XPS peak of potassium could be observed. Contact with CO_2 atmosphere at a temperature higher than 650°C is required to form potassium oxide on the surface of carbon, which can be measured by the XPS technique, but contact with O_2 at room temperature is sufficient to take potassium back to the surface from the bulk. Therefore CO_2 chemisorption at 250°C provides just the measurement of the elemental potassium embedded in the bulk carbon, instead of potassium oxides on the surface. However, as discussed earlier, one would expect that dispersion of potassium would be independent of catalyst loading on high-surface-area substrates (35) and at relatively low catalyst loadings (36). From these two aspects, it can be understood why, in the study of Illán-Gómez *et al.* (8, 33), a constant CO_2/K_2O was obtained. In the present study, KNO_3 instead of K_2CO_3 was used, and heat treatment was conducted at 500°C, at which it is impossible to produce elemental potassium. So we obtained good information about K_xO_y dispersion by CO_2 chemisorption, which is confirmed by the decreasing specific acitivity of the catalyst with increasing K loading (Fig. 6b).

In Fig. 6c, normalized Arrhenius plots by CO_2 chemisorption show that all reaction rates fall on the same line. This clearly shows that a close relationship exists between the external area (available to CO_2 chemisorption) and the catalytic activity. The activity of a catalyst in the gasification of a given carbon depends mainly on its nature, its concentration, and its dispersion in the carbon matrix, as well as on the catalyst–carbon interface. According to the literature (8, 32), CO_2 is chemisorbed on the available external surface instead of on the interfacial surface (catalyst–carbon contact). For catalytic activity, the catalyst–carbon contact is of much more importance than its available external surface area, but these two parameters must be related (32). The following model presents a good illustration for such a relationship in the case of K catalyst.

A Conceptual Reaction Model

Based upon the above discussion, with reference to Cazorla-Amorós and co-workers' model of CaO particles (37) as well as the model of Illán-Gómez *et al.* of K_xO_y particles (8), the following mechanistic model is proposed to explain the N_2O–carbon reaction catalyzed by potassium (Fig. 11).

After a 500°C heat treatment, a potassium oxide particle is loaded in carbon in the form of K_xO_y, the surface of which is divided into three zones (Fig. 11a): (I) zone A, the interface with the carbon; (ii) zone B, the perimeter of zone A, and (iii) zone C, the external surface of K_xO_y without any contact with carbon. Generally, zones B and C are available to CO_2 chemisorption or to N_2O dissociative chemisorption. By using such a three-zone K_xO_y model, the TPR process is explained as follows:

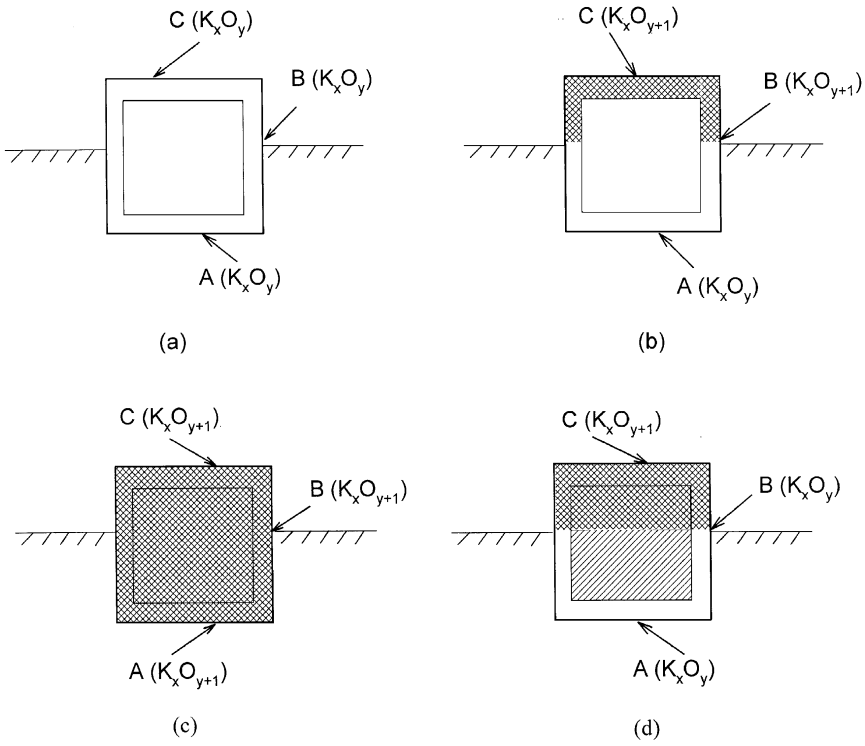

FIG. 11. A conceptual three-zone model for oxygen transfer during the reaction: (a) different zones that can be differentiated for K_xO_y particles supported on carbon, (b–d) interpretation of N_2O dissociative chemisorption and oxygen transfer during TPR.

(i) At low temperatures ($T < 50°C$), when N_2O is introduced, both zone B and zone C dissociatively chemisorb N_2O and are oxidized into K_xO_{y+1} (Fig. 11b). This chemisorption proceeds very easily and reaches saturation even at very low temperatures. Once saturation is reached, chemisorption stops. However, oxygen transfer is impossible at such low temperatures.

(ii) Both chemisorption and oxygen transfer benefit from high temperatures. When temperature rises to a certain level (ca. 150°C for K20/AC), oxygen accumulated on B and C during the first stage can gradually migrate into the bulk or even to the interface of the potassium oxide particle. This makes zone B and C less oxidized, so continuous N_2O chemisorption on B and C begins to proceed again. At ca. 250°C, the whole particle is nearly oxidized into K_xO_{y+1} (Fig. 11c).

(iii) A further increase in temperature makes oxygen transfer possible from K_xO_{y+1} to carbon. This occurs on the catalyst–carbon contact—zones B and A. As the oxygen close to the carbon active sites has priority for transfer, an oxygen gradient is formed in the reaction process (Fig. 11d): at the catalyst contact (zones B and A) is K_xO_y; at the external surface (zone C) is K_xO_{y+1}. Oxygen can diffuse from a high concentration area to a low concentration area. At the same time, part of N_2O can also diffuse from zone B to zone A, and from zone C to zone B, leaving part of zone B and C less occupied by N_2O. The N_2O on the catalyst–carbon inteface is beneficial to the removal of surface carbon–oxygen complexes through the formation of CO_2 instead of CO and through making the chemisorption of CO_2 on potassium oxide particles less stable. The oxygen gradient in potassium oxide particles is maintained through the release of carbon–oxygen complexes, and the N_2O–carbon reaction catalyzed by potassium can proceed continuously.

Based on the above model, the available surface area measured by CO_2 chemisorption is actually the surface for N_2O dissociative chemisorption, and the carbon–catalyst interface is vital for oxygen transfer from K to carbon. For the potassium catalyst, once oxygen transfer starts, its rate increases much more quickly than that of the dissociative N_2O chemisorption, which is demonstrated by the quick excess of oxygen-containing products with respect to N_2 in the TPR experiments. This means that when temperature reaches a certain level, the conversion rate of N_2O is limited by chemisorption not oxygen transfer. That is why, although the CO_2 chemisorption is not a measurement of catalyst–carbon contact area or active sites, the amount of CO_2 adsorbed presents excellent normalization in Fig. 6c.

CONCLUSION

N_2O conversion to N_2 over activated carbon can be substantially catalyzed by potassium, which proves to be much more active than copper and cobalt. Potassium possesses stronger abilities for N_2O dissociative chemisorption and oxygen transfer compared with copper and cobalt. Moreover, potassium also shows advantages of stability and flexibility in catalyst preparation, and the nature of redispersion of potassium in carbon proves to play a critical role.

A detailed study of the reaction mechanism was conducted based upon three different potassium loadings. An analysis of products during TPR provides very useful information. It is found that the negative oxygen balance at low temperatures (<50°C) is due to the oxidation of the external surface of K_xO_y particles. With the increase in temperature, the bulk or even the catalyst–carbon interface of catalyst particles is also oxidized gradually. The release of carbon–oxygen complexes from the carbon surface maintains the oxygen gradient in the catalyst particles, thus N_2O-carbon reaction catalyzed by potassium can proceed continuously. N_2O is beneficial to the removal of carbon–oxygen complexes through both the formation of CO_2 instead of CO and the destabilization of CO_2 chemisorption on K_xO_y particles. A three-zone model was proposed and successfully used to elucidate the mechanism of N_2O–carbon reaction over K/AC catalysts. CO_2 chemisorption at 250°C proves to be effective for the measurement of K dispersion.

ACKNOWLEDGMENTS

Financial support from the TIL program, Department of Education, Commonwealth Government of Australia, is gratefully acknowledged. The authors also thank Dr. N. Pollack of Calgon Carbon Corp. for supplying the activated carbon samples.

REFERENCES

1. McKee, D. W., *in* "Chemistry and Physics of Carbon" (P. L. Walker, Jr., and P. A. Thrower, Eds.), Vol. 16, p. 1. Dekker, New York, 1988.
2. Pullen, J. R., *in* "Catalytic Coal Gasification," IEA Report ICTIS/TR 26. International Energy Agency, Coal Research, London, 1984.
3. Mims, C. A., *in* "Fundamental Issues in Control of Carbon Gasification Reactivity" (J. Lahaye and P. Ehrburger, Eds.), p. 383. Kluwer, Dordrecht, 1991.
4. Kapteijn, F., and Moulijn, J. A., *Fuel* **62**, 221 (1983).
5. Moulijn, J. A., and Kapteijn, F., *in* "Carbon and Coal Gasification" (J. L. Figueiredo and J. A. Moulijn, Eds.), p. 181. Nijhoff, Dordrecht, 1986.
6. Kapteijn, F., Alexander, J. C., Mierop, G. A., and Moulijn, J. A., *J. Chem. Soc. Chem. Commun.*, 1084 (1984).
7. Okuhara, T., and Tanaka, K., *J. Chem. Soc. Faraday Trans.* **82**, 3657 (1986).
8. Illán-Gómez, M. J., Linares-Solano, A., Radovic, L. R., and Salinas-Martínez de Lecea, C., *Energy Fuels* **9**, 97 (1995).
9. Illán-Gómez, M. J., Linares-Solano, A., Radovic, L. R., and Salinas-Martínez de Lecea, C., *Energy Fuels* **9**, 104 (1995).
10. Pels, J. R., Ph.D. thesis, Chaps. 5–6, Delft University of Technology, 1995.
11. Thiemans, M. H., and Trogler, W. C., *Science* **251**, 932 (1991).
12. Li, Y., and Armor, J. N., *Appl. Catal. B* **1**, L21–29 (1992).
13. Zeng, H. C., Lin, J., Teo, W. K., Wu, J. C., and Tan, J. C., *J. Mater. Res.* **10**, 545 (1995).
14. Kinzig, A. P., and Socolow, R. H., *Phys. Today* **47**, 24 (1994).

15. Kapteijn, F., Rodriguez-Mirasol, J., and Moulijn, J. A., *Appl. Catal. B* **9**, 25 (1996).
16. Zhu, Z., Lu, G. Q., Zhuang, Y. H., and Shen, D. X., *Energy Fuels* **13**, 763 (1999).
17. Smith, R. N., Lesnini, D., and Mooi, J., *J. Phys. Chem.* **61**, 81 (1957).
18. Rodriguez-Reinoso, F., Garrido, J., Martin-Martinez, J. M., Molina-Sabio, M., and Torreogrosa, R., *Carbon* **27**, 23 (1989).
19. Garrido, J., Linares-Solano, A., Martin-Martinez, J. M., and Rodriguez-Reinoso, F., *Langmuir* **3**, 76 (1987).
20. Kodama, C., Orita, H., and Noaoye, H., *Appl. Surf. Sci.* **121/122**, 579 (1997).
21. De Rossi, S., Ferraris, G., and Mancini, R., *Appl. Catal.* **38**, 359 (1988).
22. Hu, Y. H., and Ruckenstein, E., *J. Catal.* **172**, 110 (1997).
23. Mims, C. A., and Pabst, J. K., *ACS Preprints Div. Fuel Chem.* **25**, 258, 263 (1980).
24. Mims, C. A., and Pabst, J. K., *Fuel* **62**, 176 (1983).
25. Radovic, L. R., Walker, P. L., Jr., and Jenkins, R. G., *Fuel* **63**, 1028 (1984).
26. Spiro, C. L., McKee, D. W., Kosky, P. G., and Lamby, E. J., *Fuel* **63**, 133 (1984).
27. Kapteijn, F., Abbel, G., and Moulijn, J. A., *Fuel* **63**, 1036 (1984).
28. Chen, S. G., and Yang, R. T., *J. Catal.* **138**, 12 (1992).
29. Chen, S. G., and Yang, R. T., *J. Catal.* **141**, 102 (1993).
30. Ruckenstein, E., and Hu, Y. H., *Ind. Eng. Chem. Res.* **36**, 2533 (1997).
31. Ratcliffe, C. T., and Vaughn, S. N., *ACS Preprints Div. Fuel Chem.* **30**, 304 (1985).
32. Linares-Solano, A., Almela-Alarcón, M., and Salinas-Martínez de Lecea, C., *J. Catal.* **125**, 401(1990).
33. Illán-Gómez, M. J., Linares-Solano, A., Radovic, L. R., and Sallinas-Martínez de Lecea, C., *Energy Fuels* **9**, 104 (1995).
34. Yokoyama, S., Tanaka, K., Toyoshima, I., Miyahara, K., Yoshida, K., and Tashiro, J., *Chem. Lett.*, 599 (1980).
35. Hippo, E. J., Jenkins, R. G., and Walker, P. L., Jr., *Fuel* **65**, 776 (1986).
36. Linares-Solano, A., Salinas-Martínez de Lecea, C., Cazorla-Amorós, D., Joly, J. P., and Charcosset, H., *Energy Fuels* **4**, 467 (1990).
37. Cazorla-Amorós, D., Linares-Solano, A., and Salinas-Martínez de Lecea, C., *Carbon* **29**, 361 (1991).